



THEMIS observations of a hot flow anomaly: Solar wind, magnetosheath, and ground-based measurements

J. P. Eastwood,¹ D. G. Sibeck,² V. Angelopoulos,³ T. D. Phan,¹ S. D. Bale,^{1,4}
 J. P. McFadden,¹ C. M. Cully,^{5,6} S. B. Mende,¹ D. Larson,¹ S. Frey,¹ C. W. Carlson,¹
 K.-H. Glassmeier,⁷ H. U. Auster,⁷ A. Roux,⁸ and O. Le Contel⁸

Received 30 January 2008; revised 6 March 2008; accepted 12 March 2008; published 25 April 2008.

[1] The THEMIS spacecraft encountered a Hot Flow Anomaly (HFA) on the dusk flank of the Earth's bow shock on 4 July 2007, observing it on both sides of the shock. Meanwhile, the THEMIS ground magnetometers traced the progress of the associated Magnetic Impulse Event along the dawn flank of the magnetosphere, providing a unique opportunity to study the transmission of the HFA through the shock and the subsequent downstream response. THEMIS-A, in the solar wind, observed classic HFA signatures. Isotropic electron distributions inside the upstream HFA are attributed to the action of the electron firehose instability. THEMIS-E, just downstream, observed a much more complex disturbance with the pressure perturbation decoupled from the underlying discontinuity. Simple calculations show that the pressure perturbation would be capable of significantly changing the magnetopause location, which is confirmed by the ground-based observations. **Citation:** Eastwood, J. P., et al. (2008), THEMIS observations of a hot flow anomaly: Solar wind, magnetosheath, and ground-based measurements, *Geophys. Res. Lett.*, 35, L17S03, doi:10.1029/2008GL033475.

1. Introduction

[2] Hot Flow Anomalies (HFAs) are disruptions of the solar wind flow, lasting a few minutes, observed in the vicinity of the terrestrial bow shock (e.g., review by Schwartz *et al.* [2000] and references therein). They are caused by current sheets, probably Tangential Discontinuities (TDs) interacting with the bow shock [Schwartz, 1995]. If the solar wind convection electric field points into the TD, ions specularly reflected at the shock are channeled back along the current sheet [Burgess, 1989; Thomas *et al.*, 1991]. This results in a hot ion population which expands, excavating the solar wind and laterally driving pile up regions and shock waves [Fuselier *et al.*, 1987; Lucek *et al.*, 2004]. Whilst the evolution of ion distributions from multi-component to a single hot component is relatively

well understood, the way in which the electrons become isotropic and thermalized has not been established [Schwartz, 1995].

[3] HFAs can generate considerable dynamic pressure fluctuations in the upstream solar wind, and it has been suggested that they have a significant impact on the magnetosphere [e.g., Sibeck *et al.*, 1999]. However, theoretical studies indicate that solar wind structure is significantly modified by its passage through the bow shock [Völk and Auer, 1974; Wu *et al.*, 1993], and it is unclear that the coherent upstream dynamic pressure variation generated by the HFA survives through the shock. To address this problem, it is necessary to study HFAs both upstream and in the magnetosheath with simultaneous observations.

[4] Although HFA signatures have been observed on both sides of the bow shock, most observations have been made with single spacecraft in the solar wind [Schwartz *et al.*, 2000]. HFAs have been observed by Cluster [Lucek *et al.*, 2004] but all the spacecraft were upstream of the bow shock. Another multipoint HFA study used Interball-1 and Magion-4, but again both spacecraft were upstream [Koval *et al.*, 2005]. Here THEMIS [Angelopoulos, 2008] observations of an HFA are presented. The THEMIS spacecraft observed an HFA on both sides of the bow shock simultaneously for the first time, and the THEMIS ground-based observatories observed the subsequent response of the magnetosphere.

2. In-Situ Observations

[5] The HFA was observed on 4 July 2007, during the first phase of the mission when the THEMIS spacecraft apogee was on the dayside and the probes were in close formation. The THEMIS spacecraft were on the inbound leg of their orbit, in the vicinity of the post-noon bow shock. As shown in Figure 1 (and Table 1), THEMIS-A and THEMIS-B were separated by approximately 2 Earth radii (R_E) along a common orbit, with the other three spacecraft more closely spaced between them. The HFA was observed by THEMIS-A at 10:26:00 UT in the solar wind; at that time the other spacecraft were in the magnetosheath.

2.1. THEMIS-A in the Solar Wind: Upstream Observations

[6] Figure 2 shows THEMIS-A data from the magnetic field experiment (FGM) [Auster *et al.*, 2008], thermal plasma instrument (ESA) [McFadden *et al.*, 2008] and search coil magnetometer (SCM) (A. Roux *et al.*, Searchcoil magnetometer for THEMIS, submitted to *Space Science*

¹Space Sciences Laboratory, University of California, Berkeley, California, USA.

²NASA Goddard Space Flight Center, Greenbelt, Maryland, USA.

³IGPP, ESS, University of California, Los Angeles, California, USA.

⁴Department of Physics, University of California, Berkeley, California, USA.

⁵LASP, University of Colorado, Boulder, Colorado, USA.

⁶Now at Swedish Institute of Space Physics, Uppsala, Sweden.

⁷IGEP, Technische Universität, Braunschweig, Germany.

⁸CETP, IPSL, Velizy, France.

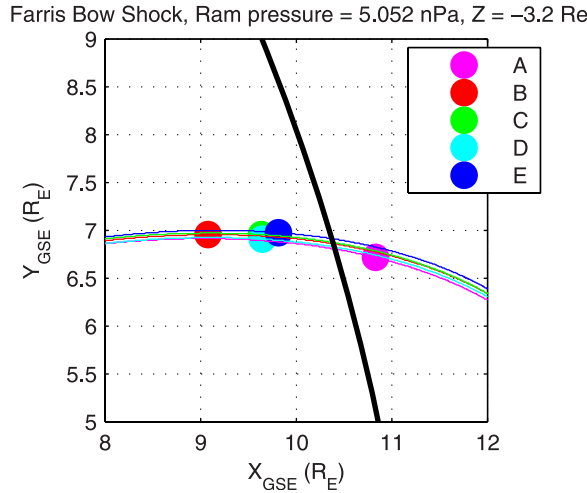


Figure 1. Location of the THEMIS probes at 10:26:00 UT are shown, in GSE coordinates (units of R_E). A model shock surface [Farris *et al.*, 1991] is shown. Only THEMIS-A was in the solar wind.

Reviews, 2008). At 10:24:50 UT, THEMIS-A crossed the bow shock (red dashed line) into the solar wind. Shortly afterwards, THEMIS-A encountered the HFA: a significant deflection in the plasma velocity, together with reduced magnetic field strength, reduced density and plasma heating was observed around 10:26:00 UT. Surrounding this central region, the plasma density and magnetic field strength were enhanced, particularly after the flow deflection was observed. The HFA lasted less than a minute, at the lower edge of typical HFA durations.

[7] The HFA was associated with a discontinuity in the interplanetary magnetic field (based on a comparison of the magnetic field orientation before and after the event), and a key formation criterion is that the solar wind convection electric field points into the underlying discontinuity on at least one side [Thomsen *et al.*, 1993; Schwartz *et al.*, 2000]. Since the EFI instrument (J. M. Bonnell *et al.*, Electric field instrument for THEMIS, submitted to *Space Science Reviews*, 2008) was not deployed on THEMIS-A, frozen-in conditions were assumed and using Minimum Variance Analysis, the convection electric field was found to point into the discontinuity on both sides with $|\mathbf{E} \cdot \mathbf{n}| = 1.9$ mV/m beforehand and $|\mathbf{E} \cdot \mathbf{n}| = 0.8$ mV/m afterwards ($\mathbf{n} = [0.952 \ 0.131 \ -0.275]$), $\lambda_{\text{int}}/\lambda_{\text{min}} = 3.6$. A more detailed analysis (not shown) shows that the structure is fairly planar. Foreshock wave activity observed between the shock crossing and the HFA indicates that the spacecraft was connected to oblique shock geometries, another important criterion [Omid *et al.*, 2007]. THEMIS-A was close to the shock and the calculated discontinuity only just intersects the model shock, suggesting that the HFA was in the early stages of its evolution, consistent with its relatively short duration.

[8] Figures 3a and 3b show 2D cuts of the 3D THEMIS-A ion distributions inside and outside the HFA, relative to the magnetic field. Outside the HFA (Figure 3b), in the solar wind, both the solar wind beam and field-aligned backstreaming foreshock ions were observed. Inside the HFA (Figure 3a), the remnant solar wind is dominated by a

sunward moving population. The presence of multiple populations is consistent with the macroscale features that suggest this HFA is relatively young.

[9] Figures 3c and 3d show similar cuts of the 3D electron distributions inside the HFA and in the solar wind. The solar wind distribution measured at 10:27:35 UT is anisotropic; $T_{\text{par}} = 1.48 T_{\text{perp}}$. Inside the HFA, at 10:26:00 UT, the electrons are observed to be essentially isotropic; $T_{\text{par}} = 0.97 T_{\text{perp}}$, as seen in other HFAs. The parallel electron plasma beta inside the HFA $\beta_{\parallel e} \sim 12$. In this regime, the electron distribution is highly constrained towards isotropy by the electron firehose instability ($T_{\text{par}}/T_{\text{perp}} > 1$) and the whistler instability ($T_{\text{par}}/T_{\text{perp}} < 1$) [Gary, 1993]. For an anisotropy $T_{\text{par}}/T_{\text{perp}} = 1.48$ at $\beta_{\parallel e} = 12$, for example, the linear growth rate of the electron firehose instability $\gamma \sim 0.1 |\Omega_e|$ [Gary and Nishimura, 2003] where the electron cyclotron frequency $\Omega_e = 351 \text{ s}^{-1}$ if $|B| = 2 \text{ nT}$ (at the center of the HFA). Thus, this instability will rapidly ($\gamma \sim 35 \text{ s}^{-1}$) render the distribution isotropic. Figure 2g shows that wave activity is suppressed at the center of the HFA, consistent with the fact that high electron beta instabilities will rapidly damp such fluctuations.

2.2. Magnetosheath Observations

[10] Magnetosheath observations from THEMIS-E (closest to the shock) are shown in Figure 4. Between 10:25:55 UT and 10:28:25 UT THEMIS-E observed a complex series of plasma structures containing flow deflections, density cavities, and hot plasma. This interval can be divided into four sections. In interval 1, there are correlated (fast mode) fluctuations in n and $|B|$. During interval 2, anti-correlated (slow mode) variations in n and $|B|$ are accompanied by significant plasma heating and a flow deflection. During interval 3, the magnetic field changes orientation several times and there is a cavity in $|B|$. Finally, in interval 4, n and $|B|$ again exhibit correlated (fast mode) enhancements.

[11] The dynamic plasma pressure is reduced during intervals 1 and 2; in fact, a simple pressure balance calculation shows that the resulting subsolar magnetopause radius would move from 8 R_E to 9 R_E each time. Interval 3 shows that the original underlying discontinuity has split into a much more complex structure. It would appear that the region of flow deflection and heating has become decoupled from the discontinuity. The presence of fast mode perturbations at the edges, particularly on the leading edge, is consistent with theoretical expectations. The slow mode rarefaction behind the leading fast mode perturbation is not predicted by theory, but was observed in a recent study comparing ACE observations of a solar wind discontinuity far upstream with Polar magnetosheath observations [Maynard *et al.*, 2007].

[12] THEMIS-C and -D (closely separated), near THEMIS-E (cf. Figure 1), observed some plasma heating and a drop

Table 1. Locations of the THEMIS Probes at 10:26 UT

Probe	[X, Y, Z] R_E (GSE)
A	[10.86, 6.74, -3.47]
B	[9.11, 6.98, -3.09]
C	[9.66, 6.98, -3.23]
D	[9.67, 6.93, -3.22]
E	[9.84, 7.00, -3.29]

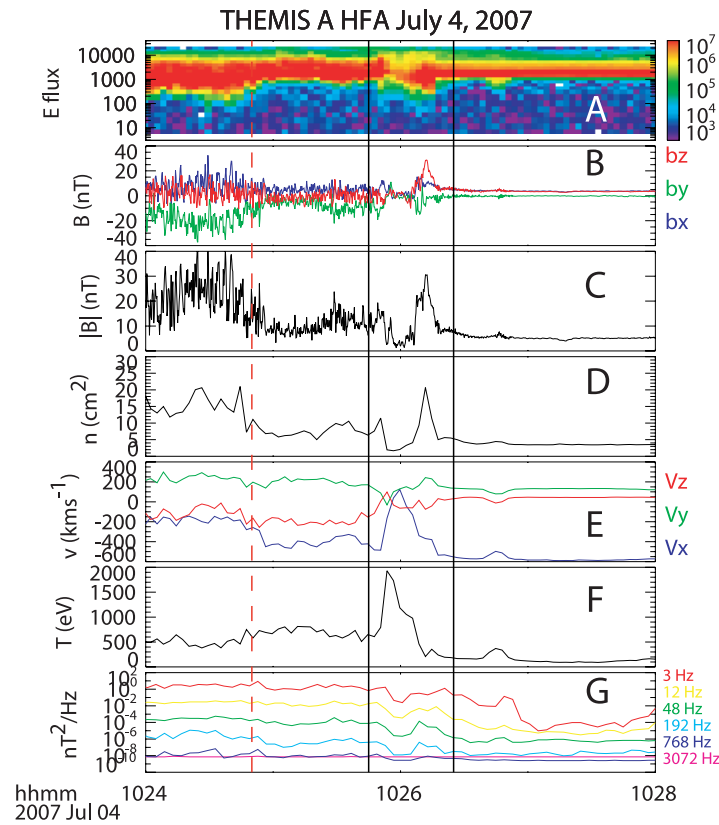


Figure 2. THEMIS-A data. (a) Ion differential energy flux ($\text{eV}/(\text{cm}^2 \text{ s ster eV})$) between 10 eV and 20 keV. (b, c) Magnetic field components in GSE and strength (d, e, f) Ion plasma density, velocity and average temperature. (g) Magnetic field fluctuations from filter bank data. THEMIS-A crossed the bow shock at 10:24:50 UT (red dashed line) and encountered the center of the HFA at 10:26:00 UT. Black vertical lines mark the extent of the HFA.

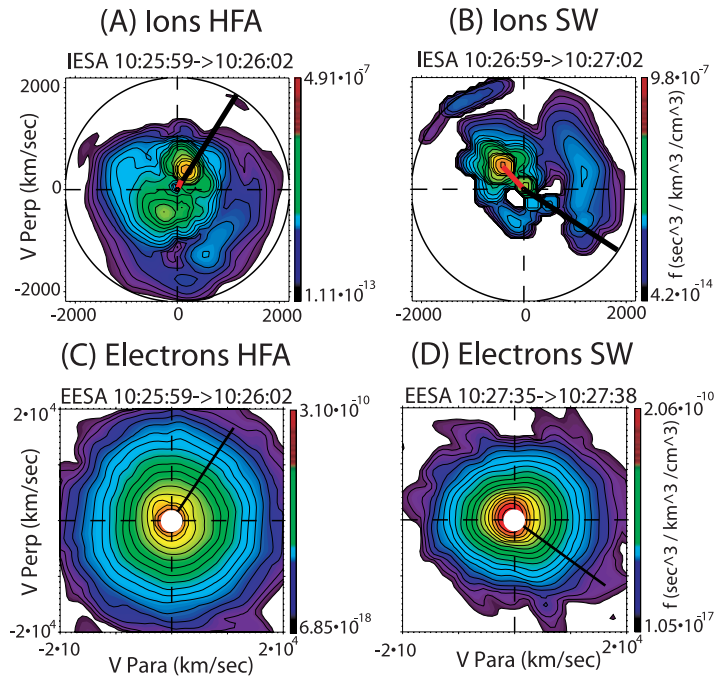


Figure 3. 2D cuts of the ion and electron plasma distributions recorded by THEMIS-A at the center of the HFA and in the solar wind. The data are shown in magnetic field coordinates. The thick black line points in the $+x_{\text{GSE}}$ direction. In the ion distributions, the thick red line points to the distribution maximum.

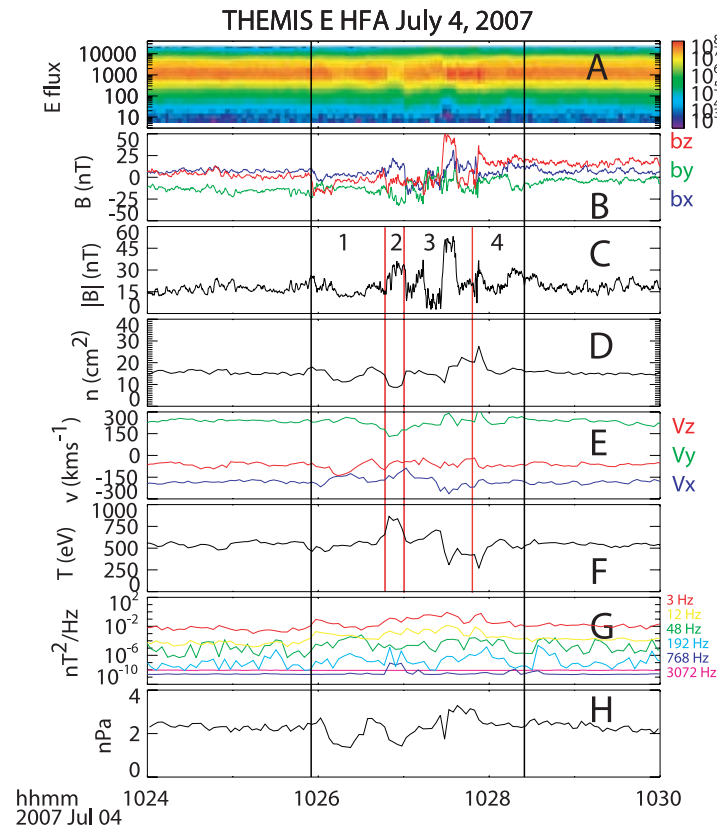


Figure 4. THEMIS-E data. (a) Ion differential energy flux ($\text{eV}/(\text{cm}^2 \text{ s ster eV})$) between 10 eV and 20 keV. (b, c) Magnetic field components in GSE and strength (d, e, f) Ion plasma density, velocity and average temperature. (g) Magnetic field fluctuations from filter bank data. (h) dynamic + thermal + magnetic pressure. THEMIS-E, in the magnetosheath, encountered a complex series of fluctuations associated with the HFA.

in the field strength, surrounded by fast mode density and field enhancements. However, no significant flow deflection was observed. THEMIS-B, furthest from the shock, saw no flow deflection or heating, although there were large fluctuations in the field strength and some changes in the density in the vicinity of the central discontinuity.

3. Ground-Based Observations

[13] The absence of significant pressure variations at THEMIS-B, the spacecraft closest to the magnetopause, at first seems to suggest that the effects of this HFA dissipated in the magnetosheath with little impact on the magnetosphere. However, there was a significant global magnetospheric response to this HFA observed on the ground. Figure 5 shows B_H measured at 5 of the THEMIS ground-based observatories [Mende *et al.*, 2008]. These 5 observatories all lie at a common geomagnetic latitude (60°N) and span 87° in geomagnetic longitude. At the time of the HFA, the magnetometers were arranged on the dawn flank of the magnetosphere (note that the THEMIS spacecraft were on the dusk flank of the shock). A magnetic impulse event was observed to propagate across the chain to progressively earlier magnetic local time, consistent with an anti-sunward propagating signal. Responses were also seen in ground-based Antarctic data (A. Weatherwax, private communication, 2008) and Polar UVI images (M. Fillingim, private communication, 2008). Therefore, the effects of

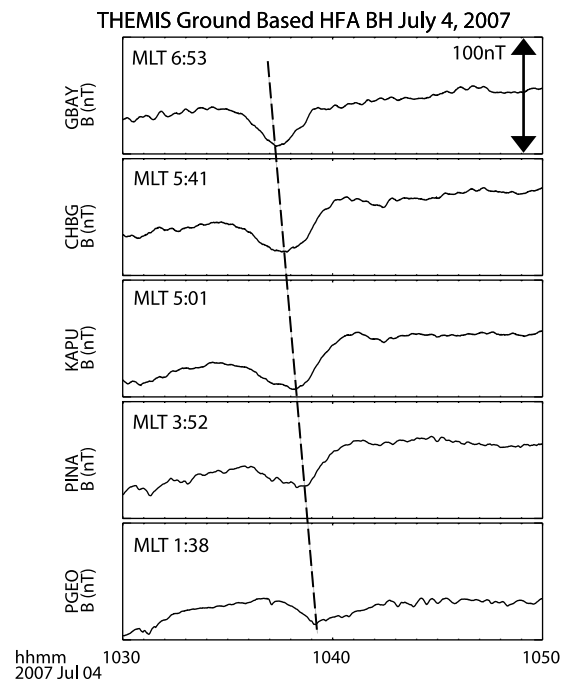


Figure 5. B_H measured at 5 of the THEMIS observatories located near 60°N geomagnetic latitude. The propagation of the MIE is marked by the dashed line.

the HFA propagated through the magnetosheath to the magnetopause.

4. Conclusions

[14] On 4 July 2007, THEMIS observed an HFA both up and downstream of the bow shock simultaneously, the first time an HFA has been captured in this way. These observations allowed the downstream structure of the HFA to be clearly identified in the context of the upstream measurements, and determine the manner in which the upstream disruption is transmitted through the shock. In addition, the THEMIS ground-based observatories showed that the HFA had a significant magnetospheric response.

[15] THEMIS-A observed classical HFA signatures upstream of the bow shock. The electrons appeared to be isotropic inside the upstream HFA because of the electron firehose instability which grows extremely quickly under the observed conditions. Downstream, at THEMIS-E, several fluctuations in the dynamic pressure were observed surrounding the discontinuity, which itself had decomposed into a series of structures. Although such step-wise magnetic field changes were observed by Šafránková *et al.*, [2002], the THEMIS multi-point observations directly show that such variation is indeed introduced at the shock rather than being a feature of the existing structure. Based on simple calculations, the observed magnetosheath pressure fluctuation was capable of significantly perturbing the magnetopause, directly confirmed by the ground-based observations.

[16] It would appear that this HFA was in the early stages of its evolution, which may explain why THEMIS-B, furthest from the shock, saw no flow deflection or heating. The geometry of the encounter suggests that the discontinuity (and thus the HFA) first touched the bow shock on the dusk flank where it was observed in-situ. The HFA is tied to the line of contact between the discontinuity and the bow shock, which moves away over the nose of the shock due to the convection of the discontinuity in the solar wind, as shown in simulations [Lin, 2002]. The absence of significant flow deflections at THEMIS-B implies it was too far away from the shock to see the young HFA, and that subsequently, the HFA moved away from the spacecraft faster than the flow disruption propagated towards the spacecraft. Conversely, the movement of the HFA across the shock enabled the transmission of the disturbance across the whole magnetosphere. Comparison with such simulations, using these data as boundary conditions, will enable a complete understanding of this event.

[17] **Acknowledgments.** This work was supported by NASA grant NASS-02099. The work of UA and KHG was financially supported by the German Ministerium für Wirtschaft und Technologie and the German Zentrum für Luft- und Raumfahrt under grant 50QP0402.

References

- Angelopoulos, V. (2008), The THEMIS mission, *Space Sci. Rev.*, in press.
- Auster, H. U., et al. (2008), The THEMIS fluxgate magnetometer, *Space Sci. Rev.*, in press.
- Burgess, D. (1989), On the effect of a tangential discontinuity on ions specularly reflected at an oblique shock, *J. Geophys. Res.*, *94*, 472–478.
- Farris, M. H., S. M. Petrinec, and C. T. Russell (1991), The thickness of the magnetosheath: Constraints on the polytropic index, *Geophys. Res. Lett.*, *18*, 1821–1824.
- Fuselier, S. A., M. F. Thomsen, J. T. Gosling, S. J. Bame, C. T. Russell, and M. M. Mellott (1987), Fast shocks at the edges of hot diamagnetic cavities upstream from the Earth's bow shock, *J. Geophys. Res.*, *92*, 3187–3194.
- Gary, S. P. (1993), *Theory of Space Plasma Microinstabilities*, Cambridge Univ. Press, Cambridge, UK.
- Gary, S. P., and K. Nishimura (2003), Resonant electron firehose instability: Particle-in-cell simulations, *Phys. Plasmas*, *10*, 3571–3576.
- Koval, A., J. Safránková, and Z. Němeček (2005), A study of particle flows in hot flow anomalies, *Planet. Space Sci.*, *53*, 41–52.
- Lin, Y. (2002), Global hybrid simulation of hot flow anomalies near the bow shock and in the magnetosheath, *Planet. Space Sci.*, *50*, 577–591.
- Lucek, E. A., T. S. Horbury, A. Balogh, I. Dandouras, and H. Rème (2004), Cluster observations of hot flow anomalies, *J. Geophys. Res.*, *109*, A06207, doi:10.1029/2003JA010016.
- Maynard, N. C., W. J. Burke, D. M. Ober, C. J. Farrugia, H. Kucharek, M. Lester, F. S. Mozer, C. T. Russell, and K. D. Siebert (2007), Interaction of the bow shock with a tangential discontinuity and solar wind density decrease: Observations of predicted fast mode waves and magnetosheath merging, *J. Geophys. Res.*, *112*, A12219, doi:10.1029/2007JA012293.
- McFadden, J. P., et al. (2008), Electrostatic analyzer for THEMIS and its inflight calibration, *Space Sci. Rev.*, in press.
- Mende, S. B., et al. (2008), The THEMIS ground based observatory, *Space Sci. Rev.*, in press.
- Omidi, N., and D. G. Sibeck (2007), Formation of hot flow anomalies and solitary shocks, *J. Geophys. Res.*, *112*, A01203, doi:10.1029/2006JA011663.
- Šafránková, J., L. Přech, Z. Němeček, and D. G. Sibeck (2002), The structure of hot flow anomalies in the magnetosheath, *Adv. Space Res.*, *30*, 2737–2744.
- Schwartz, S. J. (1995), Hot flow anomalies near the Earth's bow shock, *Adv. Space Res.*, *15*, 107–116.
- Schwartz, S. J., G. Paschmann, N. Sckopke, T. M. Bauer, M. W. Dunlop, A. N. Fazakerley, and M. F. Thomsen (2000), Conditions for the formation of hot flow anomalies at the Earth's bow shock, *J. Geophys. Res.*, *105*, 12,639–12,650.
- Sibeck, D. G., et al. (1999), Comprehensive study of the magnetospheric response to a hot flow anomaly, *J. Geophys. Res.*, *104*, 4577–4593.
- Thomas, V. A., D. Winske, M. F. Thomsen, and T. G. Onsager (1991), Hybrid simulation of the formation of a hot flow anomaly, *J. Geophys. Res.*, *96*, 11,625–11,632.
- Thomsen, M. F., V. A. Thomas, D. Winske, J. T. Gosling, M. H. Farris, and C. T. Russell (1993), Observational test of hot flow anomaly formation by the interaction of a magnetic discontinuity with the bow shock, *J. Geophys. Res.*, *98*, 15,319–15,330.
- Völk, H. J., and R.-D. Auer (1974), Motions of the bow shock induced by interplanetary disturbances, *J. Geophys. Res.*, *79*, 40–48.
- Wu, B. H., M. E. Mandt, L. C. Lee, and J. K. Chao (1993), Magnetospheric response to solar wind dynamic pressure variations: Interaction of interplanetary tangential discontinuities with the bow shock, *J. Geophys. Res.*, *98*, 21,297–21,311.
- V. Angelopoulos, IGPP, ESS, University of California, Los Angeles, CA 90095-1567, USA.
- H. U. Auster and K.-H. Glassmeier, IGEP, Technische Universität, Braunschweig, D-38106, Germany.
- S. D. Bale, C. W. Carlson, P. Eastwood, S. Frey, D. Larson, J. P. McFadden, S. B. Mende, and T. D. Phan, Space Sciences Laboratory, University of California, Berkeley, CA 94720, USA. (eastwood@ssl.berkeley.edu)
- O. Le Contel and A. Roux, CETP, IPSL, F-78140, Velizy, France.
- C. M. Cully, Swedish Institute of Space Physics, Uppsala SE-751 21, Sweden.
- D. G. Sibeck, NASA Goddard Space Flight Center, Code 674, Greenbelt, MD 20771, USA.